JOURNAL OF CATALYSIS **172,** 294–306 (1997)
ARTICLE NO. CA971873

Performance and Postreaction Characterization of γ-Mo_2N Catalysts in Simultaneous Hydrodesulfurization and Hydrodenitrogenation Reactions

Umit S. Ozkan,[1] Liping Zhang, and Paul A. Clark

Department of Chemical Engineering, Ohio State University, Columbus, Ohio 43210

Received March 12, 1997; revised August 14, 1997; accepted August 15, 1997

An unsupported γ-Mo_2N catalyst was prepared to perform simultaneous HDS of benzothiophene and HDN of indole, as well as HDS in the presence/absence of NH_3 and HDN in the presence/absence of H_2S. Pre- and postreaction catalysts were characterized using XPS, TPD, TPR, XRD, and BET techniques. While ethylbenzene was the only major hydrocarbon product from benzothiophene HDS throughout the temperature range tested (200–380°C), C_6–C_8 alkylbenzenes and alkylcyclohexanes were observed from indole HDN. The presence of sulfur compounds changed the products of indole HDN from primarily aromatics to cyclohexanes. In the presence of sulfur compounds, the product distribution from indole reaction over the Mo nitride catalysts was similar to that over a sulfided Mo/γ-Al_2O_3 catalyst. Postreaction XPS measurements showed a pronounced decrease in N content and the presence of MoS_2 over the Mo nitride surface. The findings of this study suggest that the bulk of the postreaction Mo nitride catalyst was still in the Mo_2N structure and that it acted as a support for the MoS_2 phase, which in turn, controlled the catalytic performance. © 1997 Academic Press

INTRODUCTION

Molybdenum nitride has been found to be a promising catalyst for hydrotreating (1–18), especially HDN reactions (1, 3–11, 13–18). Some of the studies related to the preparation, characterization, and reaction studies of Mo nitrides in hydrotreating catalysis have been reviewed recently (19). In contrast to the much more extensive literature that exists on hydrotreating catalysis over sulfide catalysts (20), much less information is available about the working mechanism of Mo nitride catalysts under practical hydrotreating conditions, since most of the publications reported the preliminary tests on HDN activity of nitride and carbide catalysts. A key question about the commercial application of Mo nitrides in hydrotreating is whether the Mo nitride structure is stable enough under typical hydrotreating reaction conditions, where sulfur compounds are inevitably present and the Mo sulfide phase is thermodynamically more stable (20). Although some of the more recent tests of Mo nitrides in hydrotreating reactions have been carried out with sulfur-containing mixtures (15–18), additional studies, including postreaction catalyst characterization are needed to help answer this question.

There are a few articles in the literature which report the postreaction characterization of Mo nitrides after being exposed to sulfur-containing media (2, 15, 18, 21), and there does not seem to be a general consensus about the changes taking place on the catalyst surface. X-ray diffraction patterns and laser–Raman spectra of Mo_2N catalysts which were sulfided and used in thiophene HDS for 24 h showed that the bulk structure of topotactic Mo_2N was retained and that there was no evidence of MoS_2 formation (2). The XPS measurement of a Mo_2N catalyst which was used in the hydrotreatment of a mixed feed containing N, S, O, and hydrocarbon model compounds showed the presence of small amounts of sulfide over the catalyst (15). The XPS data of Nagai *et al.* (21) for a nitrided Mo/Al_2O_3 catalyst which was used in dibenzothiophene HDS reaction showed that the surface of the spent catalyst was covered with sulfur, which caused the activity of the nitrided catalyst to approach that of the sulfided catalyst.

While differing views are reported in the literature about the changes on the catalyst surface due to sulfur exposure, the catalytic properties of Mo nitrides, in general, were found to be strongly affected by the presence of sulfur compounds. In the absence of sulfur compounds, Mo nitrides were found to be quite active for HDN and to have better C–N bond hydrogenolysis selectivities (less hydrogen consumption) than that of conventional sulfided Co–Mo or Ni–Mo HDN catalysts (1, 5, 7, 9). In the presence of sulfur compounds, however, this conclusion was no longer valid. It was reported that a Mo_2N catalyst, which showed a high initial activity for quinoline HDN, was completely deactivated after being exposed to a thiophene-containing feed for 1.5 h (9). There were also reports which showed that, in

[1] Corresponding author. E-mail: ozkan.1@osu.edu.

0021-9517/97 $25.00

the presence of H_2S, the product selectivity shifted significantly towards hydrogenation products while the activity remained constant during the HDN of pyridine (5) or HDN of quinoline (1) over Mo_2N catalysts. For quinoline HDN in the presence of sulfur compounds, product distribution approached that of a commercial sulfided Ni–Mo/Al_2O_3 hydrotreating catalyst (1) and the proposed quinoline HDN reaction network was also similar to that over the sulfide catalysts (15). For the hydrotreatment of feedstocks containing comparable amounts of sulfur and nitrogen compounds, Mo_2N catalysts did not appear to outperform commercial Ni–Mo sulfide catalysts (15–17).

While five-membered nitrogen heterocycles account for about two-thirds of the total nitrogen content in petroleum crude (20), for the Mo nitride system there are no reports on the HDN of five-membered nitrogen heterocyclic model compounds in the presence of sulfur compounds. The objective of the work presented in this article has been investigation of the HDN of indole, a typical five-membered nitrogen heterocyclic model compound, over unsupported Mo nitride catalysts. In an effort to gain insight into the reaction network and the active phase structure of these catalysts under different HDN/HDS reaction media, the reaction of indole was studied in the absence and the presence of H_2S and benzothiophene. HDS of benzothiophene in the presence versus in the absence of NH_3 was also studied. Postreaction characterization of the catalysts was performed mainly by using XPS without any air exposure. The reaction data and the postreaction characterization of the Mo_2N catalyst were also compared with those of a sulfided 20% MoO_3/γ-Al_2O_3 catalyst.

METHODS

The unsupported γ-Mo_2N catalyst was prepared by temperature-programmed reductive nitriding of ultrahigh purity MoO_3 (Alfa AESAR, 99.9995%) in a flow of pure NH_3. The loading of MoO_3 precursor was 2 g and the flow rate of ammonia was 195 cm^3(STP)/min. After a rapid heat-up of the MoO_3 sample to 325°C, a ramp rate of 0.4°C/min was used to increase the temperature to 515°C which was followed by a 1-h dwelling at this temperature. Then the sample was heated up to 700°C at a rate of 1°C/min and kept at the final temperature for 30 min. The synthesized γ-Mo_2N was then cooled down to room temperature. Following the cooling stage, the flow was switched from ammonia to helium to flush the reactor tube. Finally, the catalyst was passivated with 30 cm^3(STP)/min of 1% O_2 in He for 24 h. The catalyst was used in the reactor in powder form. Prior to all reaction studies, the catalyst was activated *in situ* at 400°C with 30 cm^3(STP)/min of H_2 for 12 h.

The sulfided 20% MoO_3/γ-Al_2O_3 catalyst used for the comparison was prepared by wet co-impregnation of γ-Al_2O_3 with aqueous solutions of ammonium heptamolybdate. Prior to the reaction studies, the catalyst was sulfided *in situ* at 400°C with 10% H_2 in H_2S for 10 h. The details of the preparation and the characterization of this γ-Al_2O_3-supported sulfide catalyst were presented previously (22, 23).

The Mo nitride catalysts were characterized using BET surface area, XRD, SEM, XPS, and temperature-programmed desorption and reduction techniques. The BET surface areas were measured with a Micromeritics AccuSorb 2100E instrument. Prior to the BET surface area measurement, the passivated γ-Mo_2N catalyst was degassed at 200°C for 12 h. XRD patterns were obtained using a Scintag PAD-V diffractometer with Cu Kα radiation ($\lambda = 1.5432$ Å). SEM images were obtained using a JEOL XPD-2500 scanning electron microscope. The X-ray photoelectron spectrometer used for this work was a V. G. ESCALAB Mark II operated at 14 kV and 20 mA with Mg Kα radiation. Binding energies were referenced to C_{1s} of 284.6 eV. The pressure at the XPS chamber was 10^{-9} Torr.

TPD/TPR experiments were performed in a built-in-house apparatus which was previously described (24). The sample was pretreated under vacuum at 200°C for 2 h for TPD and at 500°C for 1 h for TPR. After cooling to room temperature under vacuum, a 50 cm^3(STP)/min flow of helium (TPD) or 10% hydrogen in helium (TPR) was initiated over the catalyst material. The temperature was then raised linearly at 15°C/min (TPD) or 5°C/min (TPR) to 950°C. The reactor effluent composition was continuously monitored as a function of sample temperature by a mass spectrometer (Hewlett-Packard, MS Engine 5989A).

Catalytic reaction studies were carried out in a stainless steel flow system equipped with mass flow controllers for accurate flow delivery and on-line gas chromatography for feed and product stream analysis. The fixed-bed reactor was made out of 4-mm ID stainless steel tubing. The ends of the reactor tube were equipped with plug valves to allow removal of the reactor tube from the reaction system and air-free transfer to the XPS apparatus. The on-line GC (HP 5890A) was equipped with a 0.53-mm ID fused silica (HP-1) capillary column and a flame ionization detector. The products were identified by GC-MS analysis in conjunction with the injection of pure compounds. A more detailed description of the reaction apparatus has been reported previously (25).

Reaction experiments were conducted at a temperature range of 200–380°C and 100 psig (0.78 MPa) pressure with 0.023% (mol) indole and benzothiophene (BT) each in hydrogen. In the case where NH_3 or H_2S was present in the feed, their concentrations were kept at 0.475% (mol) each in H_2. The total gas flow rate was 30 cm^3(STP)/min. The catalyst loading in the reactor for each run was kept constant at 40 mg for the unsupported Mo nitride catalyst and 303 mg for the supported Mo sulfide catalyst. The different

catalyst loadings used for the nitride and the supported sulfide catalysts were to achieve the same conversion levels for a valid comparison.

It was verified, by running the experiment at several different gas flow rates, that under the conditions reported here, the reactions were controlled kinetically and were not limited by mass transfer. Also, calculations made according to Weisz–Prater criterion showed that diffusion limitations did not play a role in our system. Activity data were collected after steady state was reached (∼4 h). The criterion for steady state was established through monitoring the product distribution and the conversion level. The average of carbon balances for all reaction runs was $100 \pm 5\%$.

X-ray photoelectron spectra were taken for fresh and post-HDN and HDS reaction catalysts without air exposure. The postreaction analysis was done after the catalysts were kept on stream for 24 h. Following activation and/or reaction, the catalysts were flushed with helium at reaction temperature for 30 min and then cooled down to room temperature under He flow. The catalysts were then sealed using valves located on both ends of the reactor tube. The reactors were taken to an argon-atmosphere glove box where the catalysts were removed and were mounted to the XPS sample holders. The samples were then transferred to the XPS chamber via the sample transfer chamber which allows air-free transportation.

RESULTS

Catalyst Characterization

The BET surface areas were 93 and 165 m^2/g for the Mo nitride and the 20% MoO_3/γ-Al_2O_3 catalysts, respectively. The XRD patterns of the passivated, activated, and postindole HDN reaction Mo nitride catalysts were similar and all exhibited a predominantly γ-Mo_2N structure with small amounts of MoO_2 present.

The TPD profiles of the passivated Mo nitride catalyst are presented in Fig. 1. As shown in the figure, there is a broad N_2 desorption feature covering the range from 240 to 500°C. This feature is likely to be due to the loss of nitrogen from the surface/subsurface. The more intense N_2 desorption peak which starts around 500°C and reaches a maximum at 710°C might indicate loss of nitrogen from the catalyst lattice. The TPD profiles also showed desorption peaks of NH_3 and H_2O around 330 and 420°C, respectively. The TPD experiments were not designed to detect hydrogen elution. Therefore, no attempt was made to demonstrate the possible existence of hydrogen in the nitride matrix, as suggested in the literature earlier (5).

Based on the observations from the TPD experiments, a degassing treatment at 500°C was performed prior to the H_2 TPR experiments to remove all the adsorbed NH_3 and H_2O species. Therefore, it is expected that any NH_3 or H_2O that evolves up to 500°C during the TPR experiments is a result

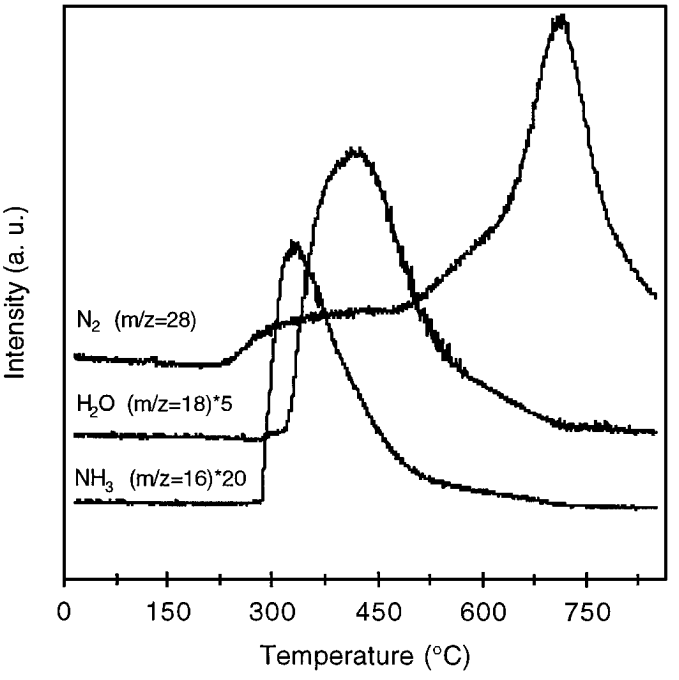

FIG. 1. TPD profiles of the passivated Mo nitride catalyst.

of the reduction reaction and is not due to the desorption of NH_3 and H_2O which are left on the surface from the preparation or from air exposure.

The results from TPR of the passivated Mo nitride are presented in Fig. 2. The H_2O signal showed a major peak

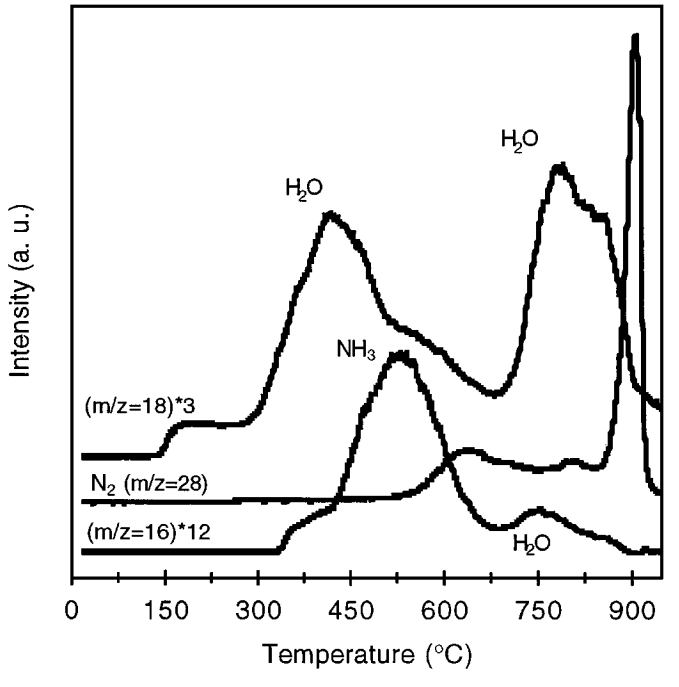

FIG. 2. H_2 TPR profiles of the passivated Mo nitride catalyst.

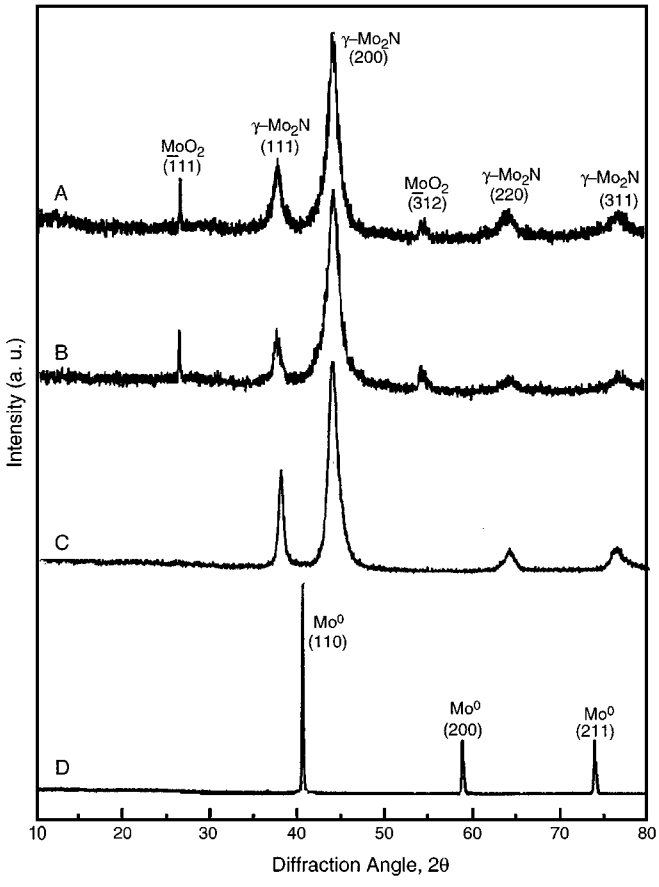

FIG. 3. XRD patterns of the Mo nitride catalyst: (A) after passivation; (B) after H_2 activation at 400°C; (C) after H_2 TPR to 795°C; (D) after H_2 TPR to 950°C.

with a maximum temperature around 410°C and a shoulder between 130 to 300°C. There was a second H_2O evolution peak with an onset temperature of 680°C and a maximum temperature of 790°C. The H_2 TPR also featured an NH_3 peak with an onset temperature of 420°C and a maximum temperature of ca 530°C. At the same temperature (ca 530°C), where ammonia evolution reached the peak maximum, N_2 evolution began and continuously gained intensity. There was a second small N_2 feature between 700 and 840°C. These first two N_2 features were much smaller than the N_2 peak which started at 840°C. The intensity of this N_2 peak reached a maximum around 910°C and went down to baseline at 950°C.

To determine the catalyst phase structure during and after the H_2 TPR, X-ray diffraction experiments were performed over the two post-TPR catalyst samples. The first sample was subjected to TPR up to 795°C; then the reduction process was interrupted and the catalyst was taken to the XRD chamber. The XRD pattern of this sample showed that the structure of the catalyst was still γ-Mo_2N, but the MoO_2 impurity had disappeared. The second XRD experiment was carried out over the catalyst which had completed the reduction at 950°C. The XRD pattern of this sample showed the characteristics of Mo metal. The XRD patterns of the Mo nitride catalyst after passivation, after H_2 activation at 400°C, after H_2 TPR to 795°C, and after H_2 TPR to 950°C are shown in Fig. 3.

When the XPS result of the passivated Mo nitride catalyst is examined (Fig. 4), it is found that the surface mainly consisted of Mo_2N and MoO_3. The observed Mo^{6+} shoulder has exactly the same $Mo_{3d_{3/2}}$ B.E. at 235.5 eV which we obtained previously for MoO_3 in both γ-Al_2O_3 supported (22, 23) and unsupported (26) Mo catalysts. The $Mo_{3d_{5/2}}$ B.E. for the Mo nitride is 228.8 eV, which is the same as in MoS_2 (23, 26).

Based on the XRD and XPS results, it can be concluded that the first water signal observed at 410°C in the TPR profile corresponds to the removal of the oxygen in the oxide layers formed during passivation and air exposure. The second major H_2O feature at 790°C, on the other hand, can be concluded to correspond to the H_2 reduction of the MoO_2 phase, which was left behind from the synthesis procedure. The ammonia peak at 530°C could be attributed to the H_2 reduction of Mo nitride, starting with the surface. As noted earlier, the nitrogen signal begins to rise as the ammonia signal reaches a maximum and starts to decrease. According to our previous ammonia TPR results (24), NH_3 begins to decompose to H_2 and N_2 when $T \geq 500$°C. Therefore, it is very likely that the first N_2 peak which starts to gain intensity as the NH_3 signal begins to subside is due to the decomposition of NH_3 formed during the reduction and it reaches a broad maximum at ca 640°C. The second small N_2 evolution feature between 700 and 840°C, according to the TPD results in Fig. 1, could be assigned to the

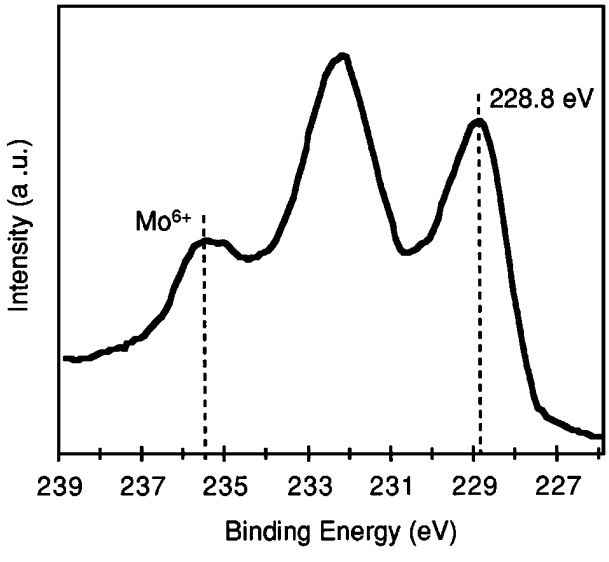

FIG. 4. XPS spectra of the Mo_{3d} region for the passivated Mo_2N catalyst.

loss of lattice nitrogen by heating. After this N_2 evolution, the catalyst still maintains the γ-Mo_2N structure, as seen in X-ray diffraction, although it is highly probable that the partial loss of nitrogen from the lattice could be forming some vacancies or more accurately nitride phases with varying stoichiometries. The strong N_2 evolution peak at 910°C is clearly due to the complete transformation of the Mo_2N phase into Mo metal phase, as seen in the post-TPR X-ray diffraction pattern. SEM images obtained from this sample showed a highly porous, sponge-like structure.

Reaction Studies

Activity and product distribution in HDS and HDN over molybdenum nitride. The reaction data were expressed in terms of observed conversion rate and observed product formation rates, all in the units of 10^{-9} moles per minute per m^2 of catalyst, [nmol/(min · m^2)]. The conversion rate is defined as the number of moles of reactant converted per unit time per unit surface area of the catalyst. For the unsupported Mo nitride catalyst, the feed rates for both BT and indole were around 80 nmol/min · m^2. For the alumina-supported Mo/catalyst, the feed rates of the heteroatom compounds were 6 nmol/min · m^2.

Benzothiophene HDS over the γ-Mo_2N catalyst produced predominantly ethylbenzene (EB) and very small amounts of ethylcyclohexane (ECH). S-containing intermediates during BT HDS included 2,3-dihydrobenzothiophene (DHBT) and trace amounts of 2-ethylthiophenol. Figure 5 depicts the BT conversion rate as well as EB and DHBT production rates under the conditions, where BT was fed alone or co-fed with NH_3 or indole. Also shown in this figure is the variation of these rates with temperature. At 200°C the BT conversion rate was relatively low and DHBT appeared to be the major product. When the temperature was increased to 260°C, BT desulfurization was nearly complete and the EB production rate was close to the BT conversion rate in the absence of NH_3 or indole.

At temperatures ≤260°C, the presence of NH_3 in the feed resulted in a lower BT conversion rate and much higher DHBT and thus lower EB production rates. The influence of NH_3 on BT reactivity was insignificant when $T \geq 320$°C. However, it is worth mentioning that, while some ECH was produced (~1%) in the absence of NH_3, the selectivity towards EB was almost 100% in the presence of ammonia. The inhibition effect of indole on BT conversion was more severe than that of NH_3 and was significant for temperatures up to 320°C. DHBT was detected even at 380°C for simultaneous HDS of BT and HDN of indole.

The major N-containing intermediates that appeared during the HDN of indole were indoline (HIN) and C_6–C_8 *o*-alkylanilines. When comparing the indoline/indole mole ratio with that of theoretical thermodynamic equilibrium calculations (27), it was found that, the indoline/indole mole ratio was less than the equilibrium value when H_2S was not present and was close to that value when H_2S was present.

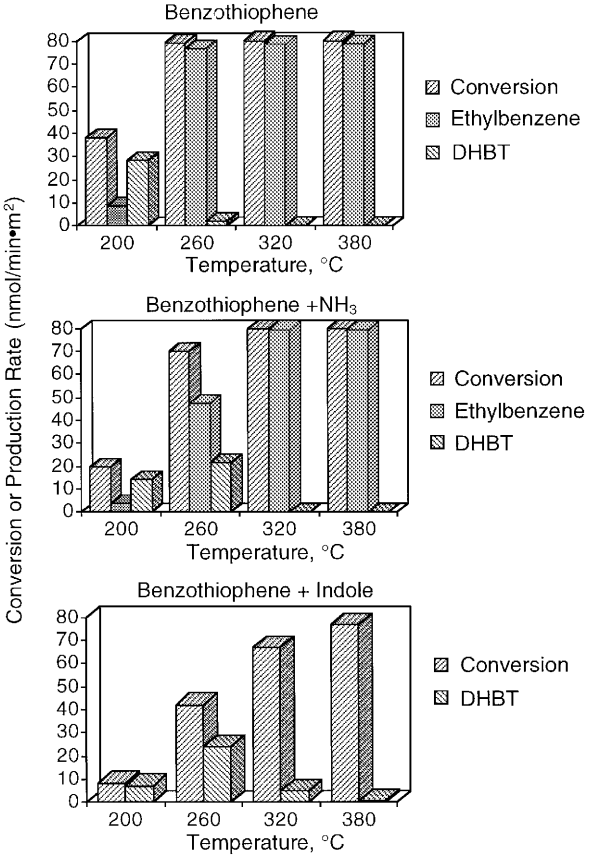

FIG. 5. Benzothiophene conversion rate and product formation rates over the Mo_2N catalyst for three different reaction media: 0.023% BT; 0.023% BT + 0.475% NH_3; 0.023% BT + 0.023% indole.

The hydrocarbon products of indole HDN observed in this work include mainly C_6–C_8 alkylbenzenes, alkylcyclohexanes, alkylcyclohexenes, and trace amounts of alkylcyclopentanes and *o*-xylene. The distribution of products was found to be a strong function of reaction media and temperature. The formation rates of hydrocarbon products from indole HDN in the presence of benzothiophene were estimated by deducting those which result from benzothiophene HDS. It is assumed that the hydrocarbons from BT HDS were 99% ethylbenzene and 1% ethylcyclohexane.

Figure 6 shows the variation of indole conversion rate and HDN rate with temperature in three different reaction media. The most important observation from this figure is that the indole HDN rate was much lower than its conversion rate in almost every case. As seen in the figure, the Mo_2N catalyst did not show appreciable denitrogenation activity at temperatures ≤320°C. Nearly complete nitrogen removal was observed only in the absence of sulfur compounds at 380°C. The presence of H_2S resulted in a slightly higher HDN rate at temperatures ≤320°C, but a significantly lower HDN rate at 380°C. The presence of the same

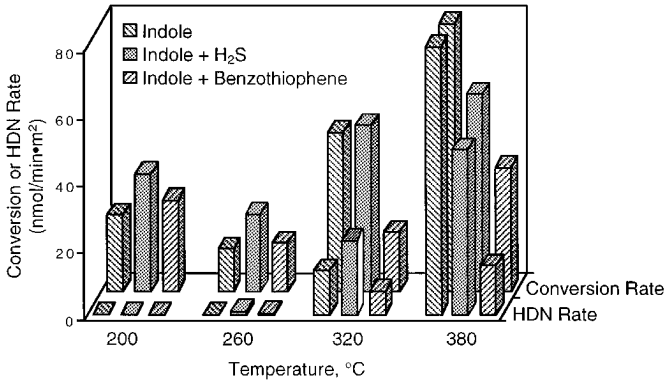

FIG. 6. Indole conversion and HDN rates over the Mo_2N catalyst for three different reaction media: 0.023% indole; 0.023% indole + 0.475% H_2S; 0.023% indole + 0.023% BT.

concentration of benzothiophene with indole appeared to have a severe inhibition effect on indole HDN at all temperatures tested.

Figure 7 shows the effect of reaction media on the extent of saturation of the hydrocarbon products from indole HDN, by comparing the production rates of three aromatics (benzene, toluene, and EB) versus total hydrocarbons (C_{6+}) at two different temperatures. In the absence of sulfur compounds, the rate for aromatics was only slightly lower than that of the total hydrocarbons. However, in the presence of sulfur compounds the production rate of aromatics was much lower than that of the total hydrocarbon products, indicating extensive hydrogenation of the benzene ring of indole under these conditions.

Figure 8 shows the distribution of the three major aromatic products (benzene, toluene, ethylbenzene), and the three cyclohexanes (cyclohexane, methyl cyclohexane, ethylcyclohexane), from indole conversion in three different reaction media at 320 and 380°C. At 320°C, EB was the major unsaturated product regardless of the reaction media. At 380°C, however, the trend was different, depending on the medium. While EB still had the highest formation rate among the three aromatics when H_2S or BT was present, both toluene and benzene showed higher production rates than EB in the absence of sulfur compounds, with toluene becoming the major product. When the production rates of alkylcyclohexanes, i.e., cyclohexane, methylcyclohexane, and ethylcyclohexane, are compared for the

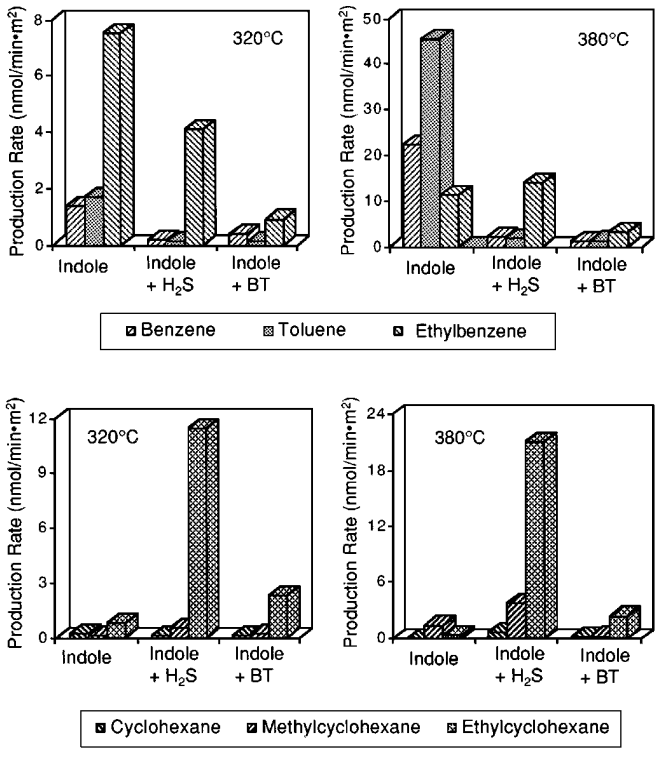

FIG. 8. Variation of the production rates of the major unsaturated and saturated hydrocarbons with reaction media from indole HDN at 320 and 380°C over the Mo nitride catalyst.

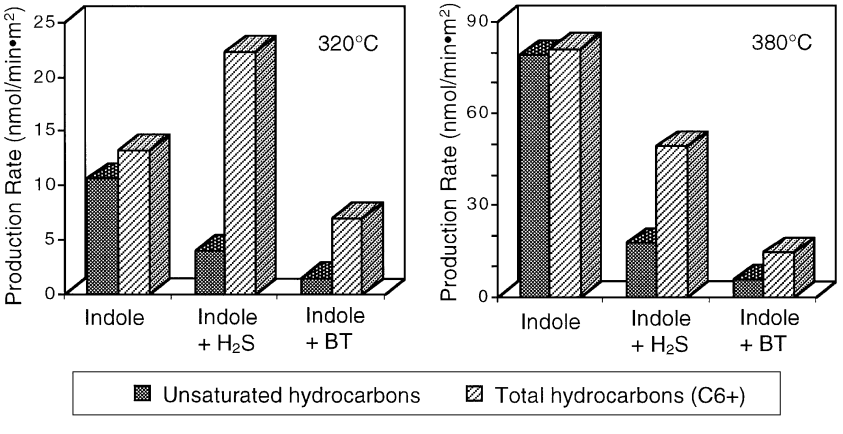

FIG. 7. Variation of the production rates of the unsaturated hydrocarbons and total hydrocarbons (C_{6+}) with reaction media from indole HDN at 320 and 380°C over the Mo nitride catalyst.

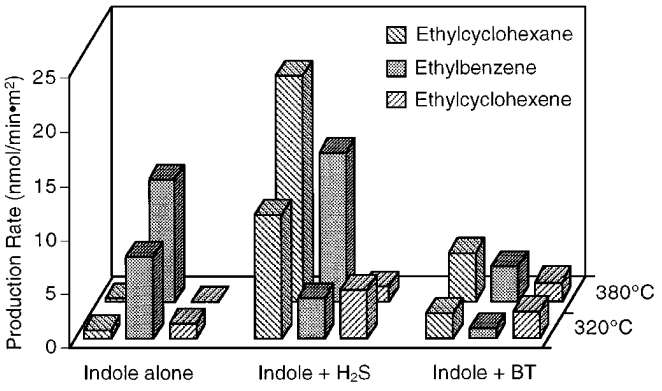

FIG. 9. Variation of the three C_8 hydrocarbon production rates with reaction media from indole HDN at 320 and 380°C over the Mo nitride catalyst.

three different reaction media, it is seen that these products were important only when sulfur compounds are present and ECH was the predominant alkylcyclohexane product among them.

Figure 9 shows the distribution of the major C_8-hydrocarbon products, i.e., ECH, EB, and ethylcyclohexene (ECHE), from indole HDN in different reaction media. As seen previously, the presence of sulfur compounds increases the extent of saturation, resulting in not only much higher yields of ECH than EB, but also in significant levels of ECHE, especially at the lower temperature. At 320°C, ECHE was among the final products, even in the absence of sulfur compounds.

Significant amounts of aniline-type nitrogen compounds were observed in the reactor effluent of indole HDN whenever the conversion of indole was not complete. Figure 10 compares the aniline, *o*-methylaniline (OMA), and *o*-ethylaniline (OEA) production rates for three different reaction media at three different temperatures. As shown in the figure, while OEA consistently had the highest yield among the three anilines, the production rate of OMA remained significant at every condition, and even aniline was detected at nonnegligible levels under most conditions.

Comparison of the HDN product distribution over molybdenum nitride and molybdenum sulfide catalysts. The performance of the Mo nitride in indole HDN was compared with that of a sulfided 20% MoO_3/γ-Al_2O_3 catalyst. Exactly the same reaction conditions were chosen, except that the catalyst loading in the reactor was different in order to achieve similar indole conversion levels. Product selectivities in the absence of sulfur compounds at 380°C are compared in Fig. 11, where indole conversion was around 95% over both catalysts. There were two major differences in product selectivities for the two catalysts. First, the nitride catalyst exhibited a higher cracking activity as reflected by the higher selectivity towards C_7 and C_6 products. The sulfide catalyst, on the other hand, had the C_8 hydrocarbons as the major products. The amount of heavy products (C_{9+} N-containing compounds as identified by GC and GC-MS analyses) were also larger over the sulfide catalyst. Since the total amounts of C_{9+} N-containing products were small, individual quantification of each of the heavy species were not performed and they were lumped together in the calculations. Second, the selectivity toward saturated products was much lower over the nitride catalyst than it was over the sulfide catalyst. The selectivities for the cyclohexanes over the nitride and the sulfide catalysts were 2 and 17%, respectively.

When the nitride and sulfide catalysts were compared in the presence of sulfur compounds, however, the findings were very different from those obtained in the absence of sulfur compounds. Figures 12 and 13 compare the distribution of major C_6–C_8 products from indole reaction in the presence of H_2S over the Mo nitride and the Mo sulfide catalysts, at 320 and 380°C, respectively. The indole

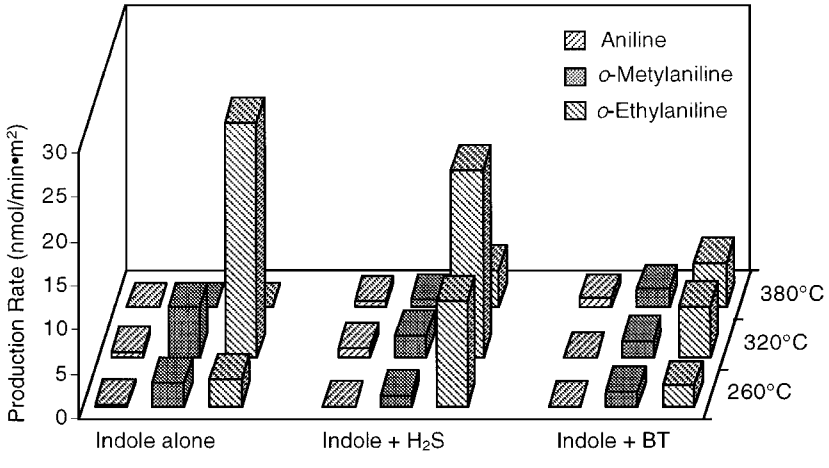

FIG. 10. Variation of the production rates of anilines with reaction media from indole HDN at 260, 320, and 380°C over the Mo nitride catalyst.

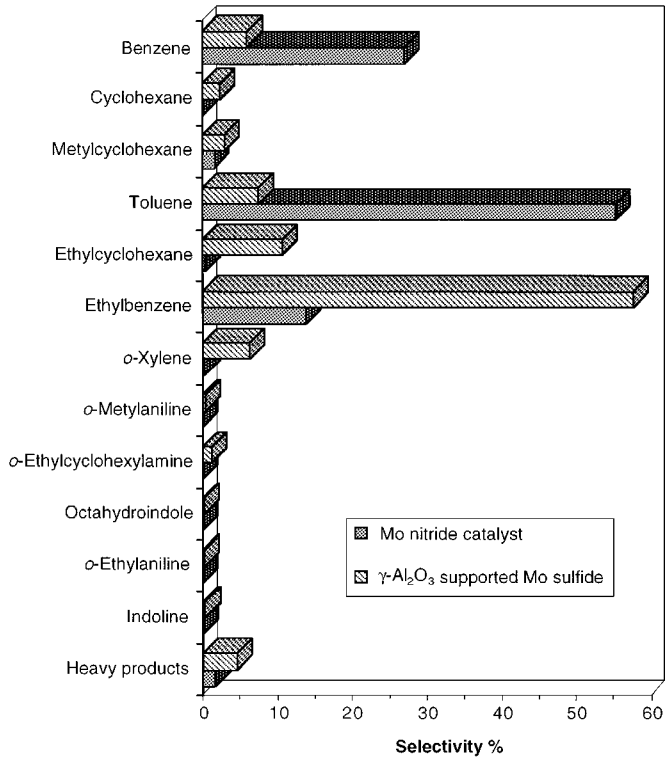

FIG. 11. Comparison of the indole reaction product selectivities at 380°C over the Mo_2N and the sulfided 20% MoO_3/γ-Al_2O_3 catalyst in the absence of sulfur compounds.

conversion level for the two catalysts was again comparable, being around 60% at 320°C and around 80% at 380°C. Once steady state was reached, the product distributions over the two catalysts were found to be very similar, as depicted in the pie graphs. The similarity in the catalytic performance of the nitride and the sulfide catalysts in the presence of H_2S was reiterated at 380°C as well as at 320°C.

Postreaction XPS Measurements

Figure 14 shows the postreaction XPS spectra of Mo_{3p}–N_{1s} region for the Mo_2N catalyst after activation (Fig. 14a) and after being exposed to different reaction media (Figs. 14b–e). A significant decrease in nitrogen content over the catalyst surface was observed for the samples after BT HDS, simultaneous HDS/HDN, as well as HDN in the presence of H_2S. Although much less pronounced, there was a small reduction in the N_{1s} signal, even after the catalyst was exposed to indole HDN reaction only.

Figure 15 shows the Mo_{3d} spectra and the curve-fitting results for the Mo nitride catalyst after being activated with hydrogen at 400°C and after being used for indole HDN for 24 h. Curve fitting of Mo_{3d} peaks was accomplished using linked doublets of equal FWHM, an intensity ratio of 2/3, and a splitting of 3.15 eV for the $Mo_{3d_{3/2}}$ and $Mo_{3d_{5/2}}$. The Mo_{3d} spectrum for the activated catalyst can be fitted into three doublets, with $Mo_{3d_{5/2}}$ binding energies at 228.9, 230.4, and 232.3 eV. The peaks at 228.9 and 232.4 eV correspond to molybdenum nitride and MoO_3, respectively (5). Although we believe that the signal observed at 228.9 eV represents predominantly Mo_2N, we cannot rule out the possible existence of β-$Mo_{16}N_7$ on the surface, as suggested by Choi *et al.* (5). Although the identity of the peak at 230.4 eV for Mo nitride could not be found from literature, the oxidation state of Mo at this position should be between 4+ and 6+.

In addition to those Mo species shown over the activated catalyst (Fig. 15a), one more Mo species with a $Mo_{3d_{5/2}}$

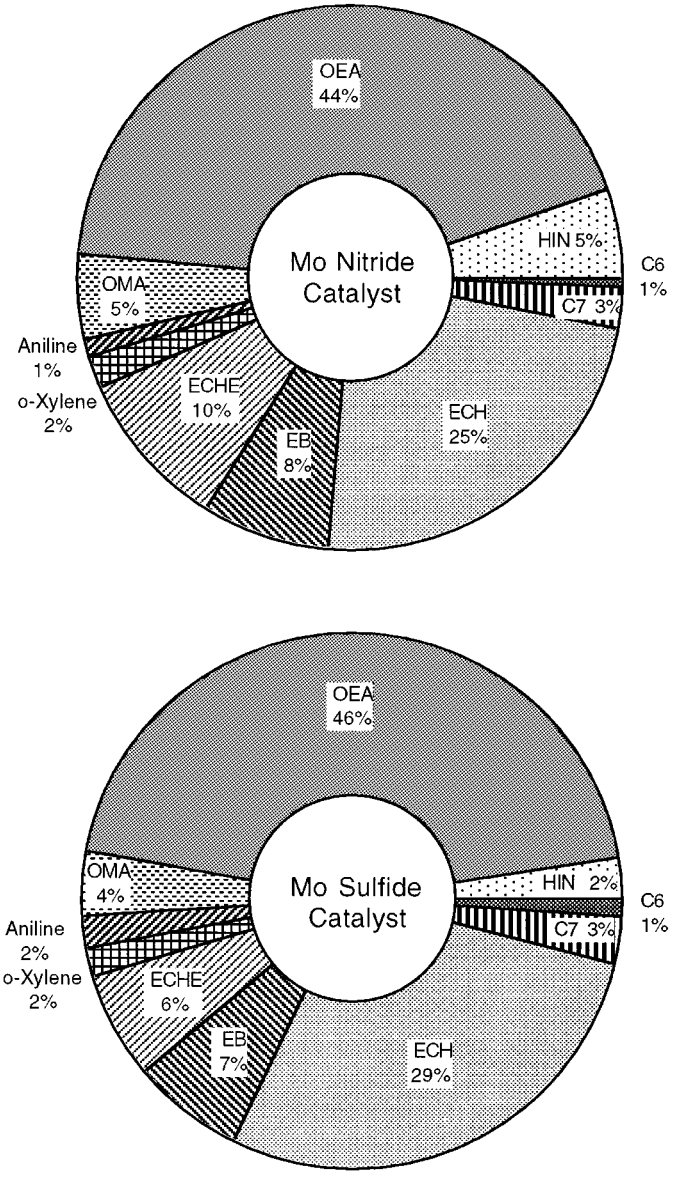

FIG. 12. Comparison of the indole reaction product distribution at 320°C over the Mo_2N and the sulfided 20% MoO_3/γ-Al_2O_3 catalyst in the presence of H_2S.

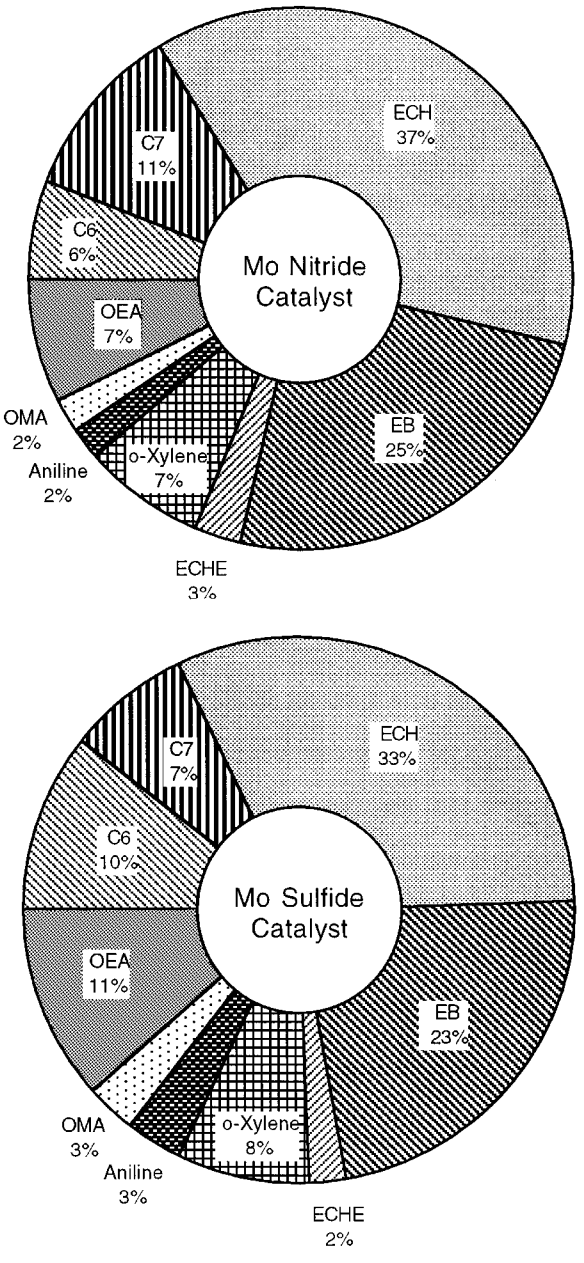

FIG. 13. Comparison of the indole reaction product distribution at 380°C over the Mo_2N and the sulfided 20% MoO_3/γ-Al_2O_3 catalyst in the presence of H_2S.

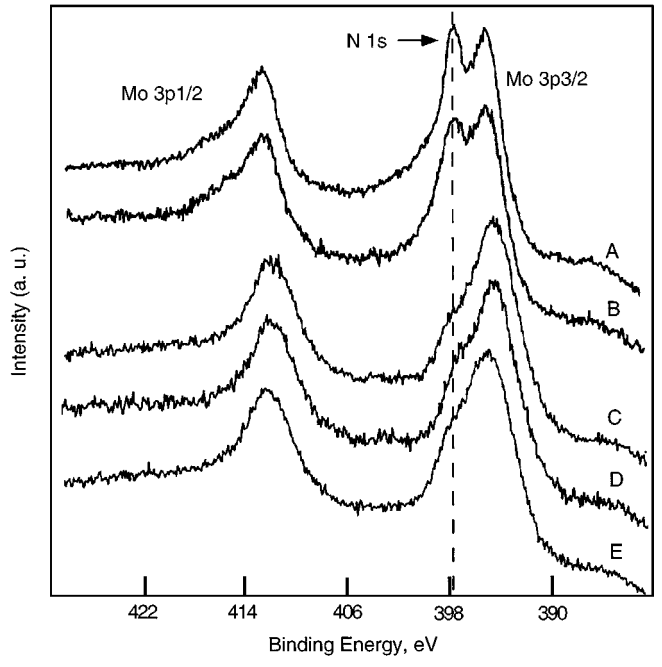

FIG. 14. XPS spectra of the N_{1s}–Mo_{3p} region for the Mo_2N catalyst: (A) after H_2 activation; (B) after indole HDN reaction in the absence of sulfur compounds; (C) after simultaneous indole HDN/BT HDS reaction; (D) after indole HDN reaction in the presence of H_2S; (E) after BT HDS reaction in the presence of NH_3.

binding energy at 227.8 eV appeared over the post-indole reaction catalyst and the intensity of this peak was relatively high (Fig. 15b). The XPS spectra of Mo_{3d}–S_{2s} region and curve fitting results for the catalyst samples which were used for HDS or HDN reactions in the presence of sulfur compounds are shown in Fig. 16. The different reaction media used were simultaneous indole HDN-BT HDS, indole HDN in the presence of H_2S, and BT HDS in the presence of NH_3. The spectra and the curve fitting results for each sample were very similar in not only the number of Mo peaks that were deconvoluted, but also in the resulting binding energies for each of the peaks obtained. While the peak at 227.8 eV was quite intensive in every sample, there was also a significant S_{2s} peak (BE = 226.3 eV) over all the catalyst samples which were exposed to sulfur-containing reaction media. When the S_{2p} region of the XPS spectra for those sulfur-exposed nitride catalysts was examined, the binding energy obtained was 162.2 eV, which corresponds to sulfur in MoS_2.

The amount of Mo in the form of MoS_2 was estimated based on the integrated peak intensities of $Mo_{3d_{5/2}}$ and S_{2p} normalized by the atomic sensitivity factors. The estimation results are listed in Table 1. The numbers in Table 1 suggest that around 14–17% of Mo in the catalysts was sulfidized after being exposed to a sulfur containing stream at 380°C for 1 day. Since the XPS penetration depth is more

TABLE 1

XPS Estimation of the Percentage Mo in the Form of MoS_2 for the Postreaction Mo Nitride Catalysts

Reaction media	$S_{2p}/Mo_{3d_{5/2}}$ [a]	% Mo in the form of MoS_2
Indole + H_2S	0.34	17%
Indole + BT	0.28	14%
BT + NH_3	0.29	15%

[a] Normalized intensity ratio.

than a monolayer thick, one can expect the percentage of the sulfided molybdenum to be significantly higher in the outermost layer.

In addition to the sulfidation, the increase in the intensity of the 227.8 eV peak and the consequent decrease of the 228.9 eV peak also suggest a decrease in the amount of nitride in the surface layers. The identification of the 227.8 eV peak needs to be examined. Brainard and Wheeler reported the binding energy of Mo_2C to be 227.8 eV for $Mo_{3d_{5/2}}$ and 282.2 eV for C_{1s} (28). Thompson and co-workers, on the other hand, assigned a binding energy of 227.8 eV that they observed in the XPS spectra of their Mo nitride samples to Mo metal (5, 10). It is worth mentioning that the C_{1s} spectrum obtained for our postreaction Mo nitride catalysts showed a feature around 282.2 eV. However, it is difficult to make a definitive assignment of this peak based on the evidence that is available. It remains as a possibility that the Mo signal we observed at 227.8 eV belongs to Mo_2C. However, we cannot rule out that it may be due to Mo metal, either. It appears more appropriate at this point to assign the 227.8 eV peak to $Mo^{\delta+}$ with $\delta < 4$, corresponding to a Mo phase with a lower N coordination. This proposal is supported by the observation made in the N_{1s} signal (Fig. 14), there seems to be a correlation between the intensity of N_{1s} and the 227.8 eV peak, i.e., the higher the N_{1s} intensity, the lower the 227.8 eV peak intensity.

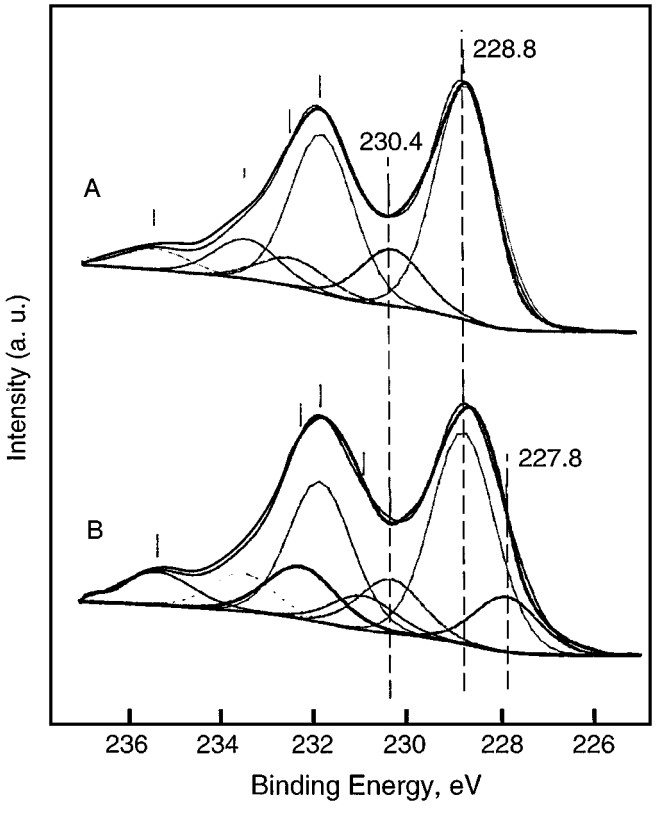

FIG. 15. XPS spectra of the Mo_{3d} region and the deconvolution results for the Mo_2N catalyst: (A) after H_2 activation; (B) after indole HDN reaction in the absence of sulfur compounds.

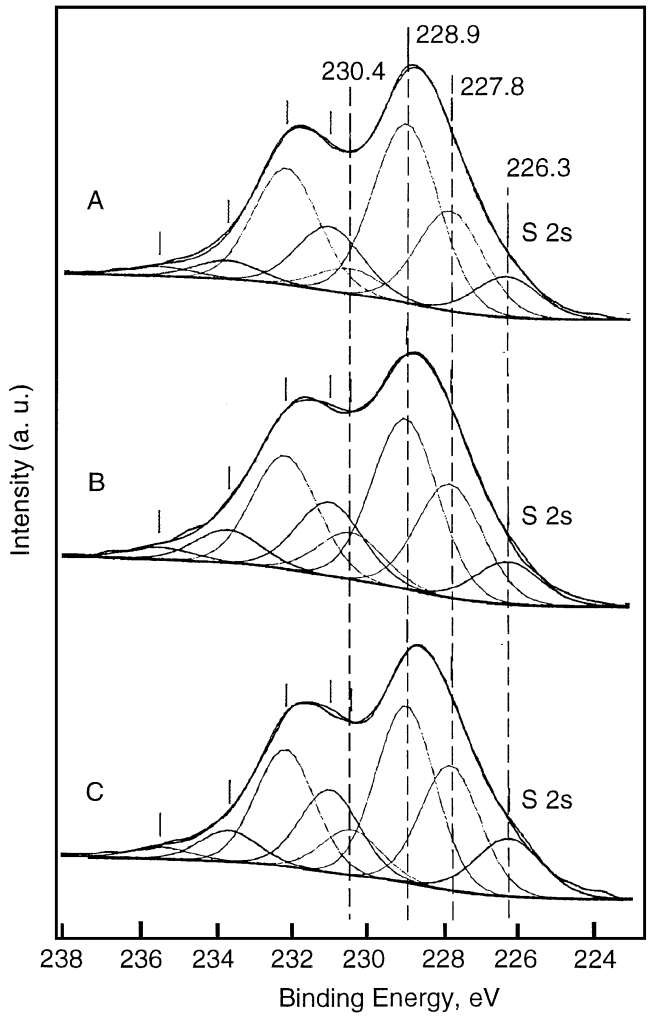

FIG. 16. XPS spectra of the Mo_{3d}–S_{2s} region and the deconvolution results for the Mo_2N catalyst after being exposed to sulfur containing media: (A) postsimultaneous HDS/HDN reaction; (B) postindole HDN reaction in the presence of H_2S; (C) post-BT HDS reaction in the presence of NH_3.

DISCUSSION

The H_2 TPR results over the passivated catalyst showed water formation at a temperature as low as 130°C. This observation indicates that the removal of the oxide layer formed during the passivation step can be readily achieved by the activation procedure of this study, i.e., flowing pure H_2 at 400°C for 12 h. Also, the fact that the catalyst was degassed at 500°C prior to the TPR procedure ensures that the water signal observed as low as 130°C was not adsorbed water, but water formed during the reduction process.

Combining the TPR results which showed the formation of NH_3 at temperatures as low as 420°C, and the post-TPR

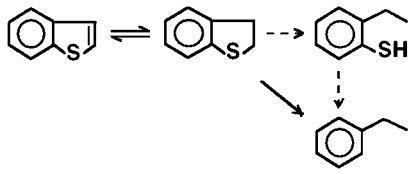

FIG. 17. Proposed benzothiophene HDS reaction network over the Mo_2N catalyst.

XRD results, which showed that the Mo_2N structure remained intact, even after reduction up to 795°C, it can be concluded that although some nitrogen was removed from the Mo nitride matrix with hydrogen, the Mo_2N structure was stable under H_2 flow up to ca 800°C. It is highly possible that the nitride structure at that point had a lower nitrogen coordination number, although there was no phase transformation that could be detected with XRD. When the reduction temperature was higher than 840°C, the Mo_2N crystal structure began to collapse under H_2 flow.

The fact that the NH_3 signal intensity increased rapidly right after the H_2O peak reached its maximum suggests that the oxide layer which resulted from passivation may retard the ammonia evolution. Therefore, after the oxide layer is removed, the reduction of N in the Mo nitride structure may occur at a lower temperature than the observed onset temperature, around 420°C from the TPR experiment. The lower nitrogen content observed over the catalyst which has been used in indole HDN at 380°C (Fig. 14) seems to suggest that the depletion of nitrogen by H_2 already starts taking place at 380°C.

The reaction network for BT HDS over the Mo nitride catalyst observed in this study is shown in Fig. 17. The hydrogenation of the heterocycle ring seems to be needed prior to the C–S bond cleavage, as suggested by the presence of dihydrobenzothiophene (DHBT) (Fig. 5). The fact that the product selectivity from BT HDS very heavily favors EB (99%) suggests that the hydrogenation of the benzene ring is not necessary for sulfur removal in this case, similar to the results obtained over the Mo sulfide catalysts (25).

The major intermediates/products from indole HDN over the γ-Mo_2N catalyst were indoline, C_6–C_8 anilines, C_6–C_8 aromatics, cyclohexanes, and cyclohexenes. The fact that appreciable amounts of aniline and OMA were among the products of indole conversion at lower temperatures ($\leq$320°C) has several implications. First, it is very likely that the production of C_6 and C_7 hydrocarbons is associated with the presence of aniline and OMA, respectively, and does not result from the dealkylation of C_8 hydrocarbons. Second, the cleavage of the first C–N bond in indoline and the two C–C bonds in the ethyl branch of OEA takes place readily over the nitride catalyst. Third, the C–N bond breakage in anilines is somewhat more difficult, especially when the temperature is not high enough. Therefore, the HDN of some of the anilines may occur via the prior hydrogenation of the benzene ring, at least partially, as in the case of the sulfide catalysts. As pointed out in the literature (29), the C–N bond cleavage via prior saturation of the benzene ring follows a β-hydrogen elimination mechanism, resulting in cyclohexenes and cyclohexanes. The detection of cyclohexenes from the indole HDN products supports the existence of the route where saturation of the benzene ring takes place prior to the C–N bond cleavage.

Figure 18 is the proposed reaction network for indole HDN over the γ-Mo_2N catalyst which can best explain the observations from the present study. In the proposed network, the first step for indole reaction is a reversible hydrogenation of the nitrogen containing ring to produce indoline. This step is controlled by thermodynamic equilibrium under most conditions. Starting from indoline, OEA is produced from the C–N bond breaking of the heterocycle ring. OMA and aniline are then produced via the dealkylation of OEA. C–N bond cleavage of the three anilines (OEA, OMA, and aniline) gives hydrocarbons with the same carbon number as the corresponding alkylanilines. The reaction pathways for the anilines are analogous to one another and can be with or without the prior saturation of the benzene ring.

At 380°C and in the absence of sulfur compounds, indole HDN reached near completion, giving aromatics almost

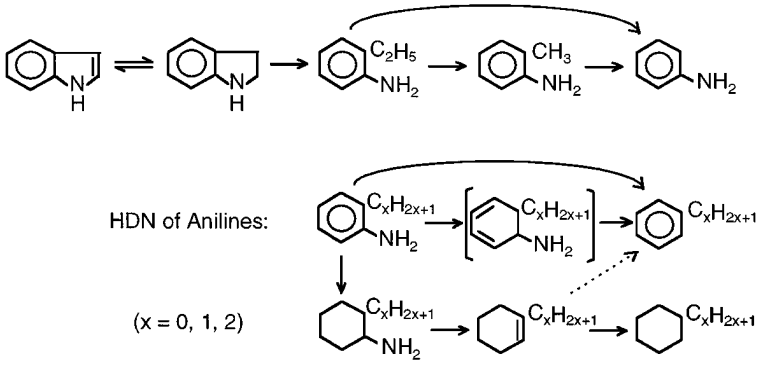

FIG. 18. Proposed indole HDN reaction network over the Mo_2N catalyst.

exclusively. This observation suggests that direct hydrogenolysis of the C–N bond in anilines may be the major route responsible for the formation of benzenes over the nitride phase at higher temperatures. Since this reaction is difficult at lower temperatures (29), it is possible that at least partial hydrogenation of the benzene ring is needed for the cleavage of the C–N bond from the anilines at lower temperatures. The low HDN activity over the nitride catalyst observed at $T \leq 320^\circ$C, coupled with the high selectivity toward aromatics seems to suggest that the Mo nitride catalyst has a relatively weak hydrogenation function, but a strong hydrogenolysis function.

Cyclohexylamines were not detected from indole HDN over the Mo nitride catalyst, indicating that either their formation is negligible or the β-elimination reaction over the Mo nitride catalysts is very fast, compared to the hydrogenation of the benzene ring. The fact that very small quantities of saturated products (cyclohexanes) were observed suggests that the formation of cyclohexylamines may indeed be negligible. It is also possible, however, that cyclohexenes via β-elimination of cyclohexylamines is preferentially dehydrogenated to give benzenes, instead of hydrogenated, to give ECH due to the weak hydrogenation function of the catalyst.

Indole HDN activity and selectivity over the Mo nitride catalyst showed significant changes in the presence of H_2S and benzothiophene. There were also important differences between the postreaction and prereaction XPS characterization of the catalysts. The implication of this observation is that sulfur compounds not only inhibited the HDN of nitrogen compounds, but they also changed the surface sites.

In order to get a comparison basis for the behavior of the nitride catalyst in the presence of sulfur compounds, the catalytic behavior of the Mo nitride catalyst was compared with that of a sulfided 20% MoO_3/Al_2O_3 catalyst. The results of this comparison are quite striking. As shown in Figs. 12 and 13, in the presence of H_2S, the product distribution from the indole reaction over the Mo nitride catalyst is almost identical to that obtained over the γ-Al_2O_3-supported Mo sulfide catalyst. The direct implication of this finding is that, in the presence of sulfur compounds, an Mo_2N-supported MoS_2 layer is formed and it plays an important catalytic role for the Mo nitride catalyst. It should be noted that the comparisons of the nitride and the sulfide catalysts in the literature were always made using the promoted (with Ni or Co) sulfide catalysts. Since the presence of Ni or Co changes the catalytic behavior of the sulfides dramatically (20, 22, 23, 25), the striking similarity in the performance of the nitride and the sulfide catalysts in the presence of sulfur compounds was never brought to light.

XRD patterns of the catalyst showed little difference between pre- and postreaction samples, suggesting the bulk structure of the Mo_2N catalyst was not affected by the reaction media, an observation made by Markel and van Zee as well (2). XPS measurements, on the other hand, showed that the nitrogen content is decreased significantly and that sulfur is present over the surface of the catalyst when exposed to sulfur-containing feed. Combining the observations from XRD and XPS experiments, it appears that there is nitrogen depletion on the surface, coupled with the formation of MoS_2 surface structures over the bulk Mo nitride phase. It is conceivable that the bulk Mo nitride phase acts as a support for the MoS_2 on the surface.

The XRD results showed the persistence of a trace amount of the MoO_2 phase after the catalyst was activated in hydrogen flow for 12 h at 400°C. There have been reports in the literature indicating that the sulfidation of MoO_2 is much more difficult than the sulfidation of MoO_3 (20, 30). Therefore, it is possible that the transformation of the MoO_2 phase to a nitride phase is also difficult.

When ammonia was included in the feed, together with BT, the postreaction XPS measurement of the catalyst indicated that NH_3 in the gas phase was not able to maintain the catalyst in its original nitride structure (Figs. 14e and 16c). This observation supports our previous premise that under the reaction conditions of this study, it is relatively easier to form a stable surface sulfide structure than it is to maintain the nitride structure even when excess amounts of NH_3 are present in the system.

CONCLUSIONS

Studies performed over a γ-Mo_2N catalyst showed appreciable activity in indole HDN and benzothiophene HDS reactions. In the absence of sulfur compounds, the products from indole HDN were primarily aromatics. In the presence of sulfur compounds, however, the major HDN products from the indole reaction were shifted from aromatics to cyclohexanes. Moreover, the product distributions over the Mo nitride catalysts were found to be essentially identical to those obtained over a sulfided Mo/γ-Al_2O_3 catalyst. Postreaction XPS measurements showed a pronounced decrease in the nitrogen content and the presence of MoS_2 on the surface, although the bulk of the catalyst was still in the Mo_2N structure. It is conceivable that the bulk Mo_2N functions as a support for the MoS_2 overlayers, which, in turn, may be changing the catalytic behavior.

ACKNOWLEDGMENTS

Financial support provided for this work by the National Science Foundation through Grant HRD-9023778 and by the EXXON Education Foundation is gratefully acknowledged.

REFERENCES

1. Schlatter, J. C., Oyama, S. T., Metcalfe, J. E., and Lambert, J. M., Jr., *Ind. Eng. Chem. Res.* **27**, 1648 (1988).

2. Markel, E. J., and Van Zee, J. W., *J. Catal.* **126**, 643 (1990).
3. Sajkowski, D. J., and Oyama, S. T., *Prepr. Am. Chem. Soci. Symp.* **35**(2), 233 (1990).
4. Oyama, S. T., *Catal. Today* **15**, 179 (1992).
5. Choi, J. G., Brenner, J. R., Colling, C. W., Demczyk, B. G., Dunning, J. L., and Thompson, L. T., *Catal. Today* **15**, 201 (1992).
6. Nagai, M., and Miyao, T., *Catal. Lett.* **15**, 105 (1992).
7. Lee, K. S., Abe, H., Reimer, J. A., and Bell, A. T., *J. Catal.* **139**, 34 (1993).
8. Abe, H., and Bell, A. T., *Catal. Lett.* **18**, 1 (1993).
9. Abe, H., Cheung, T. K., and Bell, A. T., *Catal. Lett.* **21**, 11 (1993).
10. Thompson, L. T., Colling, C. W., Choi, D., Demczyk, B. G., and Choi, J.-G., *in* "New Frontiers in Catalysis, Proc. 10th Int. Congr. Catal." (L. Guczi *et al*., Eds.), p. 941. Elsevier Science, Budapest, 1993.
11. Nagai, M., Miyao, T., Tuboi, T., and Kusagaya, T., Surface structure of molybdenum nitride and its activity for hydrodesulfurization and hydrodenitrogenation, *in* "New Frontiers in Catalysis, Proc. 10th Int. Congr. Catal." (L. Guczi *et al*., Eds.), p. 1939. Elsevier Science, Budapest, 1993.
12. Nagai, M., Miyao, T., and Tuboi, T., *Catal. Lett.* **18**, 9 (1993).
13. Colling, C. W., and Thompson, L. T., *J. Catal.* **146**, 193 (1994).
14. Lee, J. H., Hamrin, C. E., and Davis, B. H., *Appl. Catal. A General* **111**, 11 (1994).
15. Ramanathan, S., and Oyama, S. T., *J. Phys. Chem.* **99**, 16365 (1995).
16. Raje, A., Liaw, S.-J., Chary, K. V. R., and Davis, B. H., *Appl. Catal. A: General* **123**, 229 (1995).
17. Liaw, S.-J., Raje, A., Chary, K. V. R., and Davis, B. H., *Appl. Catal. A: General* **123**, 251 (1995).
18. Sajkowski, D. J., and Oyama, S. T., *Appl. Catal. A: General* **134**, 339 (1996).
19. Oyama, S. T., "The Chemistry of Transition Metal Carbides and Nitrides." Blackie Academic & Professional, Glasgow, 1996.
20. Topsøe, H., Clausen, B. S., and Massoth, F. E., "Hydrotreating Catalysis." Springer-Verlag, Berlin, 1996.
21. Nagai, M., Goto, Y., Sasuga, H., and Omi, S., *Prepr., Am. Chem. Soci. Symp.* **41**(3), 592 (1996).
22. Ozkan, U. S., Ni, S., Zhang, L., and Moctezuma, E., *Energy Fuels* **8**, 249 (1994).
23. Ozkan, U. S., Zhang, L., Ni, S., and Moctezuma, E., *J. Catal.* **148**, 181 (1994).
24. Ozkan, U. S., Cai, Y., Kumthekar, M. W., and Zhang, L., *J. Catal.* **142**, 182 (1993).
25. Zhang, L., and Ozkan, U. S., *Stud. Surf. Sci. Catal.* **106**, 69 (1997).
26. Ozkan, U. S., Zhang, L. Ni, S., and Moctezuma, E., *Energy Fuels* **8**, 831 (1994).
27. Steele, W. V., and Chirico, R. D., Topical Report for U.S. DOE, Fossil Energy, Contract 22-83FE60149, NIPER 379, Dec. 1988.
28. Brainard, W. A., and Wheeler, D. R., *J. Vac. Sci. Technol.* **15**, 1800 (1978).
29. Perot, G., *Catal. Today* **10**, 447 (1991).
30. Satterfield, C. N., "Heterogeneous Catalysis in Industrial Practice," 2nd ed., Chap. 9, p. 383. McGraw–Hill, New York, 1991.